SEISMIC SOURCE AND PATH CALIBRATION IN THE KOREAN PENINSULA, YELLOW SEA, AND NORTHEAST CHINA

Robert B. Herrmann[1], Young-Soo Jeon[1], William R. Walter[2], and Michael E. Pasyanos[2]

Saint Louis University[1] and Lawrence Livermore National Laboratory[2]

ABSTRACT

This paper focuses on the determination of seismic source parameters for earthquakes in the region surrounding the northern Yellow Sea. Broadband waveform data from the Incorporated Research Institutions for Seismology (IRIS) and the Korean Meteorological Administration (KMA) stations are used to determine moment magnitudes, source depths and focal mechanisms for these earthquakes. The seismic moments are required to calibrate the magnitude and distance amplitude corrections (MDAC) procedure for the region. The current database consists of events in northeastern China and Korea. After initial data acquisition, efforts were directed toward defining better regional models for the required theoretical Green's functions. For the events recorded in the 500 - 1000 km distance range, the regional waveforms are used to refine the initial model. For events recorded at shorter distance, especially those in Korea recorded by the KMA and the Korean Institute of Geology and Mining (KIGAM) networks, an initial reconciliation between "joint inversion of surface-wave dispersion and receiver function" models and local waveforms was prototyped to define a generic Korean crustal velocity model. Efforts are underway to acquire a continuous broadband data stream from Korea.

OBJECTIVE(S)

This effort addresses the specific problem of understanding seismic wave propagation and sources in the broad region surrounding the Korean Peninsula, the Yellow Sea and northeastern China – the region encompassing the latitudes 30 – 50 N and the longitudes 115-135 E. The unifying feature of the studies undertaken is the use of broadband waveforms . Aspects of the effort include surface-wave dispersion measurements and waveform based source parameter determination. The results of the effort will be calibrated moments and depths for ground truth catalogs and a refined crustal velocity model for use in detailed waveform analyses of regional events.

RESEARCH ACCOMPLISHED

Initial efforts were directed at the determination of earthquake source parameters whose moment magnitudes are key to calibrating MDAC for regional phases. In addition, a subset of the events studied are sufficiently constrained to permit an evaluation of candidate crustal velocity models for improved source parameter determination.

Initial Source Parameter Determination

The determination of earthquake source parameters uses two methodologies described in the Computer Programs in Seismology – 3.30 package (CPS3.30) (Herrmann and Ammon, 2002): fitting surface-wave spectral amplitude radiation patterns and broadband waveforms. The data used for Korean earthquakes are available in miniSEED from the KMA website http://www.kmaneis.go.kr/depth04_1.htm with event locations given at http://www.kmaneis.go.kr/eng/eng02.htm. Following a new event, miniSEED data are downloaded from the KMA website for all velocity sensor and accelerometer traces, converted to seismic analysis code (SAC) and deconvolved to ground velocity. Multiple filter analysis is applied to the broadband waveforms to determine the spectral amplitudes of the fundamental mode Love and Rayleigh waves. Using surface-wave eigenfunctions of the Central U.S. (CUS) model, a grid search over strike, dip, rake and depth is made for the best fitting focal mechanism; the ambiguity of fault strike and pressure and tension quadrants is resolved by comparison with bandpass filtered waveforms and/or very sharp first motion data.

Direct waveform inversion proceeds by rotating the three component deconvolved seismograms to radial, transverse and vertical components, picking the P-wave first arrival for trace alignment, the determination of the passband for the search, followed by a similar grid search. The CPS3.30 package introduced an efficient time shifting operation to overcome imperfect source parameters and the effects of an approximate crustal model. Both source determination techniques are applied because of different sensitivity to depth and because of the negative effects of ground noise when working with earthquakes with magnitudes of less than 4.0.

Table 1 and Figure 1 present the current catalog source mechanisms for the region. These earthquakes are characterized by a maximum compressive stress axis (Zoback, 1992) oriented E to ENE. With the exception of one normal faulting mechanism, the focal mechanisms are predominantly strike-slip with some thrust faulting.

The CUS model was initially used because precomputed Green's functions were available. Surprisingly the CUS model did very well in matching waveforms. A Korea specific model is being developed so that the preliminary source parameters can be refined; it is expected that the source parameters will not change signifiicantly.

Evaluation of Joint Inversion Crustal Velocity Models for Korea

Although the CUS crustal velocity model adequately modeled earthquake waveforms out to 300 km, it is not a Korea specific model basically because the depth to the Moho in the CUS model is 40 km and joint inversion of receiver functions and surface-wave dispersion for Korea indicates a crustal thickness on the order of 30 km. The utility of the CUS model lies in the fact that its upper crustal shear-wave velocities seem to be those required to define the observed surface-wave signal in the 10 – 30 period band.

Figure 2 shows the phase and group velocity dispersion data used for the joint inversion. At long periods, the Rayleigh-wave group and phase velocity values include tomographic values estimated by Harvard and Lawrence Livermore National Laboratory (LLNL). The majority of Rayleigh wave phase velocity values are obtained from a p-omega stack of teleseismic surface waves crossing the Korean peninsula. For periods of less than 10 seconds, the p-omega stack was applied to the May 29, 2004 regional earthquake signal. Rayleigh wave group velocity values for

periods of less than 10 seconds and Love group velocity values result from the application of multiple filter analysis to broadband signals of local and regional earthquakes. A tabulation of the data sets used for various joint inversions of receiver functions at Seoul National University (SNU) is given in Table 2.

Figure 3 presents the shear-wave velocity models corresponding to the various joint inversions together with the starting model, *START/start.mod*, and the reference CUS model, *CUS/dcsuq.mod*. The deeper parts of the starting and CUS models are the AK135 structure. The joint inversion models indicate a sharp Moho at a depth of about 28-30 km. The upper 1 km is characterized by a lower velocity, overlying an almost constant velocity upper crustal layer. The middle crust has a transitional velocity structure at about 15 km to an 8 km thick constant velocity layer. The upper mantle may show evidence of a low velocity zone. Except for the INVSNU inversion which was constrained by few dispersion data, the upper 10 km of the joint inversion models are similar to the CUS model. This may explain the usefulness of the CUS model for source inversion of local and regional events.

Each of the models presented is affected by the nature of the individual dispersion data sets used. The use of short period group velocity dispersion from an analysis of earthquakes at distances < 400 km, is affected by the signal spectrum and the fact that there is not a large number of wavelengths between the source and unknown origin time bias.

To visualize the consequences of these different models, a waveform inversion, with time shifts, is run for the April 26, 2004 earthquake. This earthquake was selected because of its relatively large size and because of its location on the peninsula, surrounded by KMA stations. Thus the epicenter is well constrained.

Table 3 presents the waveform inversion grid search results for three of the crustal velocity models used. A comparison of observed and predicted traces is given in Figure 4. Fits were made for the 0.02 – 0.15 Hz frequency band, and a distance dependent weighting was applied. The agreement between the observed and predicted waveforms in Figure 4 are good, although some subtle differences are seen. Comparison of the ULJ traces at 143 km, indicates that although the P-wave arrival may align, the surface-wave pulse is typically predicted later. The problem of origin time is tied up with the velocity model, but not necessarily with depth because the surface wave pulse broadens as source depth increases. It is difficult to choose among the two Korea based models, but it is comforting that a joint-inversion model using phase velocity dispersion in the 5 – 175 second period band can form the basis for waveform inversion. The application of this model at greater distances awaits data from similarly well costrained earthquakes.

Further Evaluation of Joint Inversion Crustal Velocity Models for Korea

A new technique for investigating upper crustal structure is described in a number of papers (Campillo and Paul, 2003; Shapiro et al., 2005; Ritzwoller et al., 2005). Wapenaar (2004) used the elastic wave representation theorem to provide a theoretical understanding of the procedure. Basically, noise segments of different seismograph stations are cross-correlated and stacked the result of which is a pulse that corresponds to the Green's function between the two stations for a surface application of force. The observed pulse is shaped by the power spectrum of the loading function causing the signal (Wapanaar, 2004). To avoid biases due to large amplitude signals, especially teleseisms, the favored technique is to apply a one-bit operator to the traces followed by a cross-correlation. This non-linear operation has the side effect of yielding a signal with a very peaked spectrum, which makes the determination of the group velocities difficult. We used an alternative non-linear operator. The entire series is analyzed in one-hour chunks, which are then whitened to yield a flat amplitude spectrum. Cross-correlations are then applied, and the hourly cross-correlations are stacked.

Through cooperative efforts with KMA and researchers at Seoul National University, we have acquired 83 days of continuous 20 Hz broadband data from 12 stations of the KMA network. Initial determination of inter-station Green's functions looks promising. Figure 5 shows the Rayleigh wave group velocities (orange) estimated from 50 of the 66 possible inter-station pairs. These are compared to the theoretical dispersion of the CUS and the t5.invSNU.CVEL models. The variability in dispersion along these paths is similar to that shown in Figure 2 from local earthquake data. We noted that individual dispersion curves seem shifted along the period axis with respect to one another. If we assume that a single layer over a halfspace is an adequate model for the short periods, then the layer thickess could vary by ±20 – 30 % over the southern half of the Korean peninsula. The comparison also shows that the joint inversion model can provide information about very shallow velocity structure.

CONCLUSIONS AND RECOMMENDATIONS

This study focuses on the related determination of seismic event source parameters and crustal velocity models. The testing of crustal models derived from receiver functions and surface-wave dispersion provides confidence in those models. The recent acquisition of continuous broadband waveform data from the Korean Meteorological Administration introduces new possibilities for defining the crustal velocity structure of the study area.

The initial evaluation of the technique for determining interstation Green's functions from the cross-correlation of ground noise looks promising. The path coverage should permit a unique determination of upper crustal velocities for the southern part of the Korean Peninsula. Access to more data is required to push the analysis toward longer periods and to extend the region of study outward. Since this is a new technique, the robustness of the dispersion results must be studied in detail.

REFERENCE(S)

Campillo, M., and A. Paul (2003). Long-range correlations in the diffuse seismic coda, *Science* 299: 547-549.

Herrmann, R. B. (1979). Surface-wave focal mechanisms for eastern North American earthquakes with tectonic implications, *J. Geophys. Res.* 84: 3543-3552.

Herrmann, R. B., and C. J. Ammon (2002). Computer Programs in Seismology – 3.30: Source inversion, available at URL: http://www.eas.slu.edu/People/RBHerrmann/CPS330.html, 99pp.

Ritzwoller, M.H., N.M. Shapiro, M.E. Pasyanos, G.D. Bensen, and Y. Yang (2005), Short period surface wave dispersion measurements from the ambient seismic noise in North Africa, the Middle East, and Central Asia, in current Proceedings.

Shapiro, N.M. M. Campillo, L. Stehly, and M.H. Ritzwoller, High resolution surface wave tomography from ambient seismic noise, Science, 307: (5715), 1615-1618, 11 March 2005.

Wapenaar, K. (2004). Retrieving the elastodynamic Green's function of an arbitrary inhomogeneous medium by cross correlation, *PRL* 93: 254301, 4pp.

Zoback, M. L., (1992). First and second-order patterns of stress in the lithosphere: The World Stress Map Project. *J. Geophys. Res*. 97: B8, 11703-11728.

Table 1. Focal mechanism parameters for events plotted in Figure 1.

EVENT	LAT (N)	LON (E)	H (km)	Strike	Dip	Rake	Mw
20001209	36.46	130.04	11	185	65	75	4.06
20011121	36.72	128.28	9	115	55	35	3.44
20011124	36.74	129.87	10	315	65	20	3.79
20020317	37.99	124.53	7	180	65	-120	3.72
20020708	35.85	129.76	11	125	75	10	3.63
20020723	35.57	122.18	19	120	70	25	4.9
20021209	38.86	127.26	6	295	90	-25	3.69
20030109	37.4	124.2	5	355	65	-170	3.85
20030322	34.96	124.39	14	30	80	-170	4.83
20030330	37.57	123.57	13	25	80	-155	4.61
20031012	36.95	126.51	9	25	75	-175	3.8
20030609	36	123.6	16	305	75	15	3.98
20030415	36.44	126.17	9	300	35	50	3.3
20040105	38.7	125.1	7	135	60	25	3.25
20040426	35.8	128.2	10	150	60	50	3.64
20040529	36.67	129.94	10	160	65	65	5.1
20040601	37.2	130	19	215	70	-145	3.71
20041216	41.8	127.94	8	40	70	-155	3.97

Table 2. Details of joint inversion runs showing dispersion period range and number of observations

Inversion	Number RFTN's	Rayleigh Wave Phase Velocity	Rayleigh Wave Group Velocity	Love Wave Phase Velocity	Love Wave Group Velocity
INVSNU	39	12 – 40 s (5)	10 - 70 s (21)	–	–
nnINVSNU	39	9 – 234 (362)	10 – 200 (46)	–	–
ttt.INVSNU	39	9 – 234 (371)	10 – 200 (65)	–	–
tttt.INVSNU	39	9 – 234 (497)	15 – 175 (495)	–	–
t4.INVSNU	39	9 – 234 (371)	1.2 – 200 (122)	–	1.2 – 36 (62)
t5.INVSNU	39	4 – 234 s (411)	1 – 175 s (222)	4.6 – 12 (33)	5 – 30 (31)
t5.invSNU.CVEL	39	4 – 234 s (411)	-	4.6 – 12 (33)	–

Table 3. Grid search results for the April 26, 2004 earthquake.

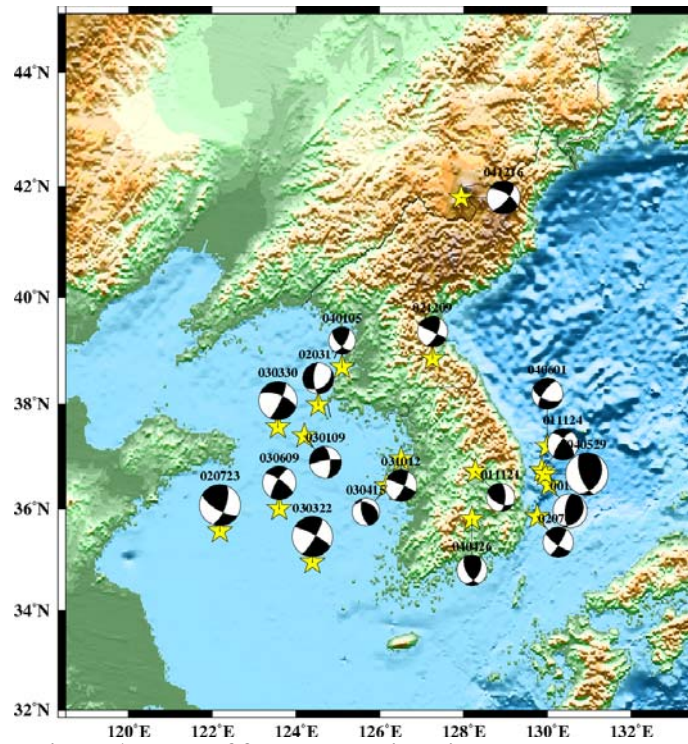| Model	H (km)	Strike	Dip	Rake	Mw	Fit
CUS	12	140	70	40	3.64	0.8088
T4.INVSNU	10	140	70	40	3.55	0.7801
T5.invSNU.CVEL	11	140	70	45	3.59	0.7748

Figure 1. Plots of focal mechanisms in the current catalog.
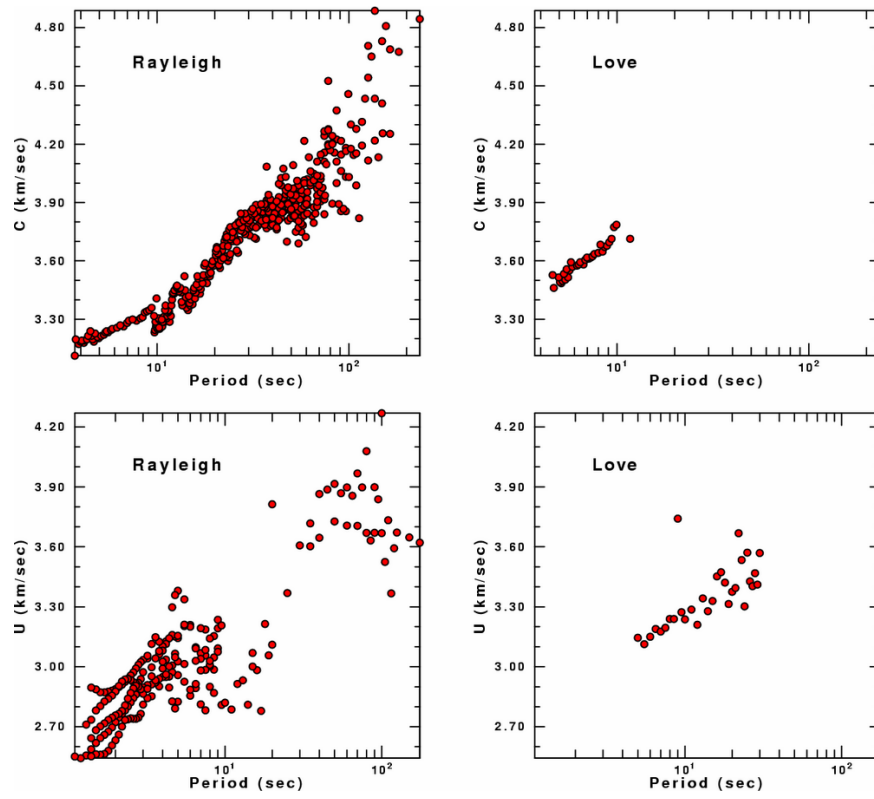
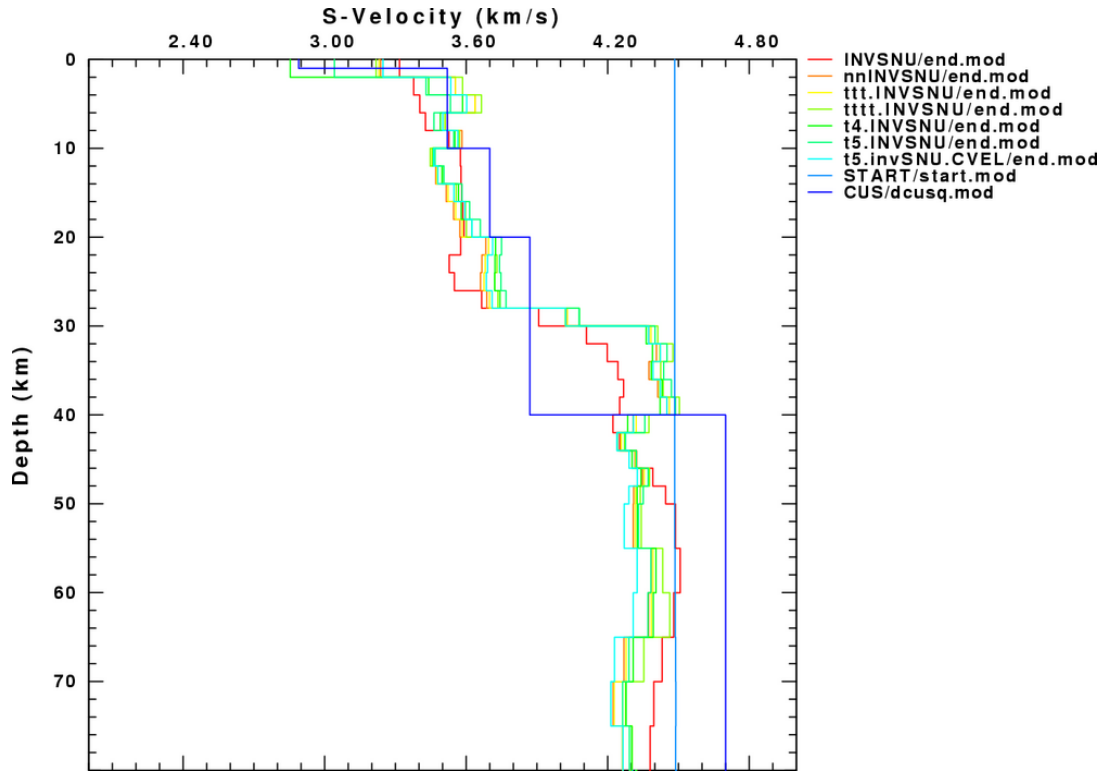**Figure 2. Dispersion values used for the t5.INVSNU and t5.inv SNU.CVEL joint inversions.**

Figure 3. Comparison of models used for synthetics. START/start.mod is the starting model.
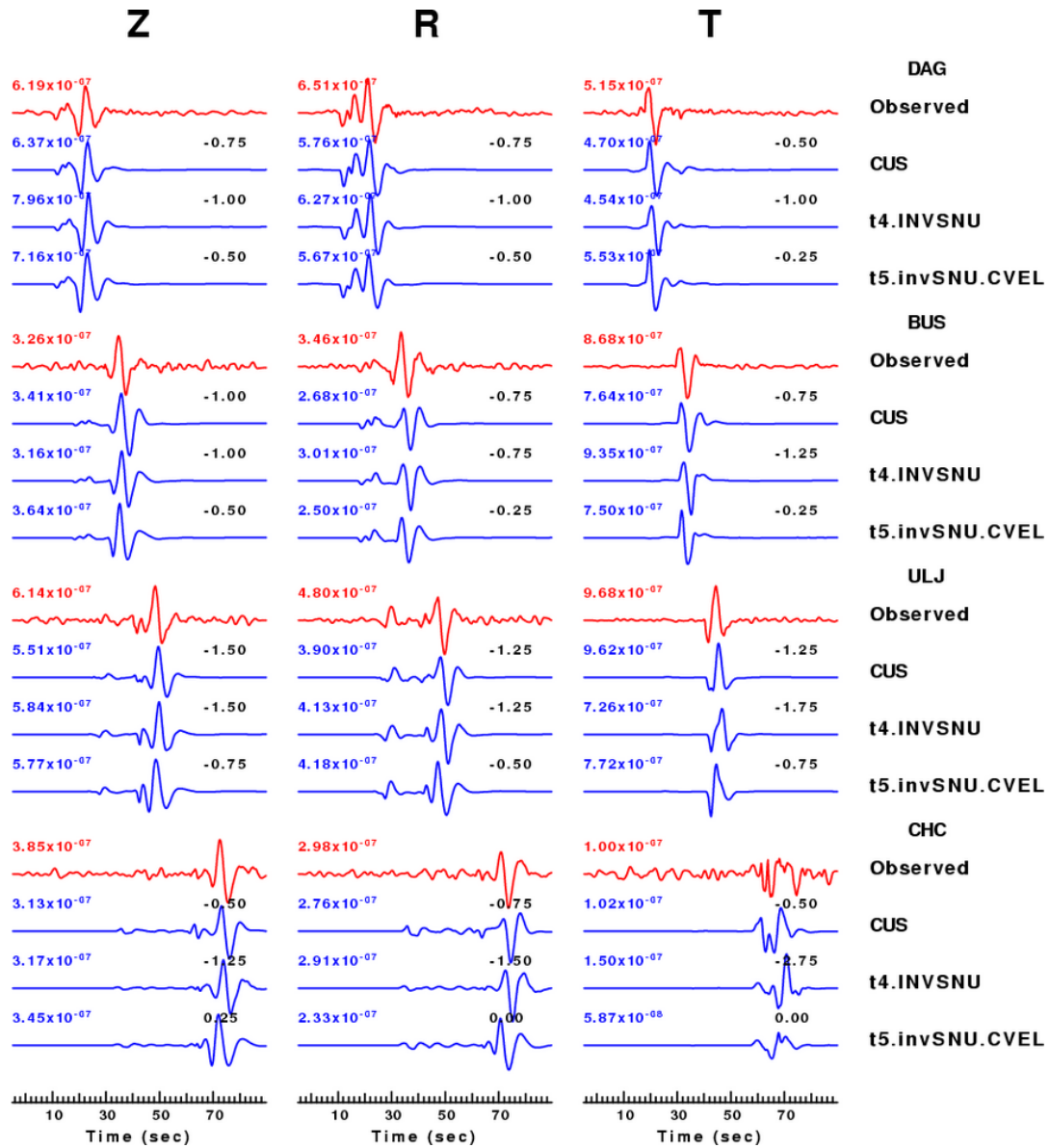
Figure 4. Comparison of observed and predicted filtered waveforms at selected stations of the KMA network for the 26 APR 2004 earthquake. The epicentral distances to the stations DAG, BUS, ULJ and CHC are 62, 104, 143 and 217 km, respectively. The observed traces are plotted in red. The number adjacent to each predicted trace is the time shift in seconds required for maximum correlation. The traces for each component of a station are plotted to the same scale. All traces start 5 seconds before and continue to 90 seconds after the origin time, and are bandpass filtered using a 3-pole high pass Butterworth at 0.02 Hz followed by a 3-pole low pass Butterworth filter at 0.15 Hz. The peak filtered amplitudes in meters/sec is indicated.
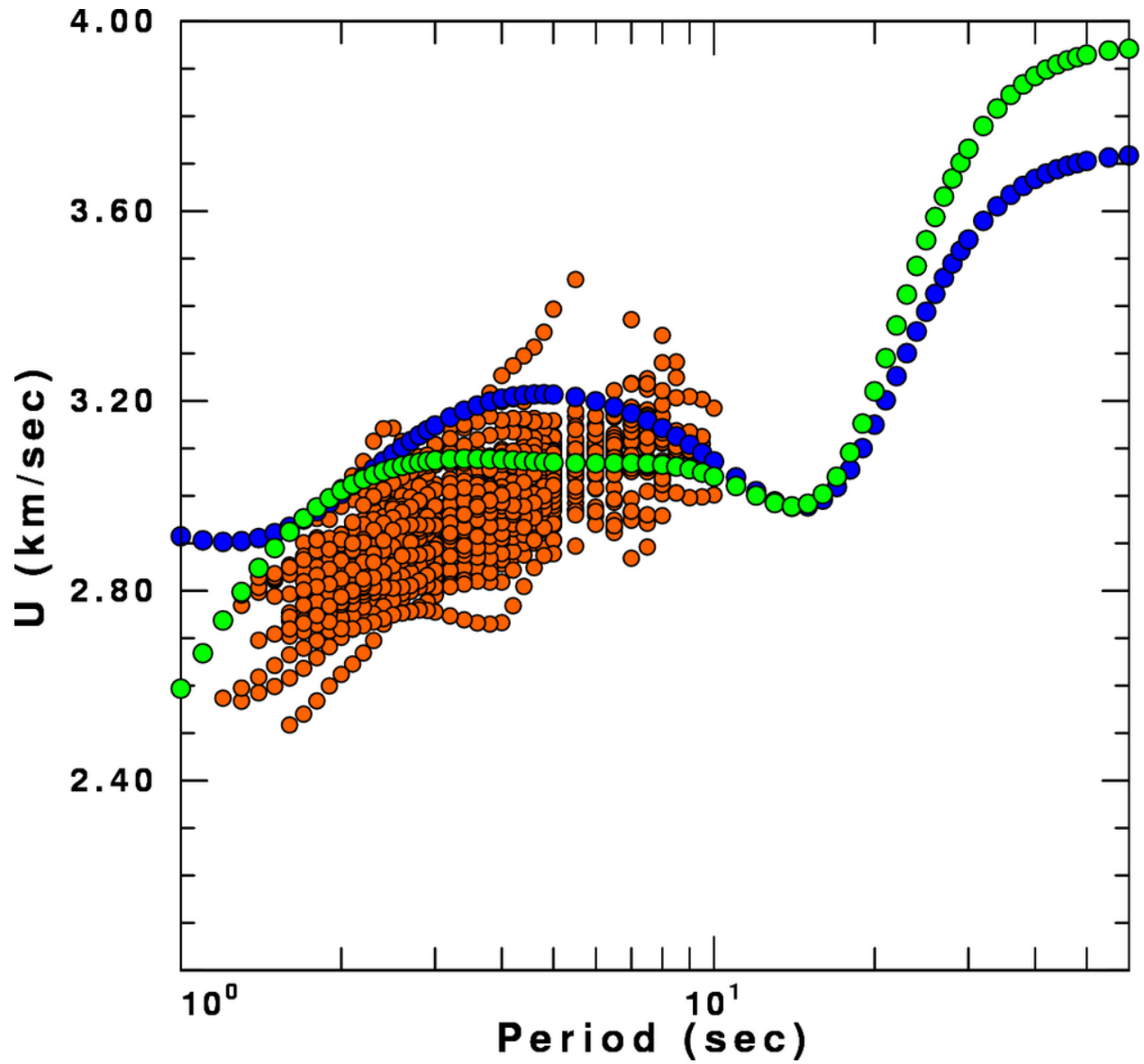
Figure 5. Comparison of interstation group velocities for station pairs in the Korean peninsula (orange) with theoretical dispersion for the CUS model (green) and t5.invSNU.CVEL (blue)